Colloids and Surfaces B: Biointerfaces 217 (2022) 112595

Contents lists available at ScienceDirect

Colloids and Surfaces B: Biointerfaces

journal homepage: www.elsevier.com/locate/colsurfb

Microgels as globular protein model systems

Natalie Nussbaum [a,1], Jotam Bergfreund [a,1], Jacopo Vialetto [b], Lucio Isa [b], Peter Fischer [a,*]

[a] Institute of Food, Nutrition and Health, ETH Zürich, Zürich 8092, Switzerland
[b] Laboratory for Soft Materials and Interfaces, Department of Materials, ETH Zürich, Zürich 8093, Switzerland

ARTICLE INFO

Keywords:
Globular Proteins
Adsorption
Fluid interfaces
Microgel
PNIPAM

ABSTRACT

Understanding globular protein adsorption to fluid interfaces, their interfacial assembly, and structural reorganization is not only important in the food industry, but also in medicine and biology. However, due to their intrinsic structural complexity, a unifying description of these phenomena remains elusive. Herein, we propose N-isopropylacrylamide microgels as a promising model system to isolate different aspects of adsorption, dilatational rheology, and interfacial structure at fluid interfaces with a wide range of interfacial tensions, and compare the results with the ones of globular proteins. In particular, the steady-state spontaneously-adsorbed interfacial pressure of microgels correlates closely to that of globular proteins, following the same power-law behavior as a function of the initial surface tension. However, the dilatational rheology of spontaneously-adsorbed microgel layers is dominated by the presence of a loosely packed polymer corona spread at the interface, and it thus exhibits a similar mechanical response as flexible, unstructured proteins, which are significantly weaker than globular ones. Finally, structurally, microgels reveal a similar spreading and flattening upon adsorption as globular proteins do. In conclusion, microgels offer interesting opportunities to act as powerful model systems to unravel the complex behavior of proteins at fluid interfaces.

1. Introduction

Globular proteins are ubiquitous, spherically-assembled biopolymers. Their amphiphilic nature drives them to adsorb to fluid interfaces, where they undergo a structural deformation due to lateral interfacial stresses and thermodynamically favorable rearrangements. Understanding protein adsorption to fluid interfaces, and the consequent assembly and refolding, is essential for the development of industrial emulsions and foams, the stability of pharmaceutical biotherapeutic formulations, the understanding of animal and human physiological mechanisms, and for many environmental processes [1–7]. However, elucidating the adsorption and reconfiguration processes is a complex task with several unresolved issues. Efforts have been made to unravel the interfacial structure and degree of unfolding with neutron reflectometry, synchrotron radiation, circular dichroism, dynamic force microscopy, molecular dynamic simulations, and interfacial rheometry [3,8–13]. These studies suggest an unfolding of globular proteins depending on the protein's internal structure and isoelectric point, ionic strength and pH of the aqueous phase, the presence of small surfactant molecules, and the properties of the hydrophobic phase. As experimental conditions may vary and the used methods are either indirect measurements or simulations, which only give access to mean properties, results reported in the beforementioned literature are partly inconsistent with each other. Therefore, a micron-sized model system, which can help further elucidate the interfacial deformation and morphology of adsorbed globular proteins, would be highly beneficial.

Microgels made of polymerized N-isopropylacrylamide (pNIPAM) were proposed as promising simplified model systems for studying protein denaturation, 3D bulk gelation [14,15] and 2D adsorption and assembly of globular proteins [16–20]. The advantage of these synthetic polymer-based microgels is their high degree of monodispersity and uniformity compared to bio-based microgels, e.g., from proteins. The behavior of pNIPAM in water is governed by the competition of the screening of the hydrophobic groups from contact with water and the presence of conformational constraints, e.g. cross-links. This competition presents analogies with the case of proteins, where their tertiary structure is determined by a complex energy landscape [21]. Typically, pNIPAM microgels swell in aqueous solutions, resulting in porous particles with a denser core structure surrounded by a softer polymer corona [22]. Upon adsorption to a fluid interface, microgels rearrange

* Corresponding author.
E-mail address: peter.fischer@hest.ethz.ch (P. Fischer).
[1] These two authors contributed equally.

https://doi.org/10.1016/j.colsurfb.2022.112595
Received 28 February 2022; Received in revised form 6 May 2022; Accepted 22 May 2022
Available online 27 May 2022

due to lateral stresses into a “fried-egg" morphology [23], similar to the interfacial reorientation of globular proteins. Finally, the adsorption and interfacial assembly of globular proteins has been shown to depend on their size, cross-linking, shape, and location of hydrophobic residues [10,24]. These factors can be accurately controlled during the synthesis of microgels, and have also been shown to affect their adsorption, interfacial assembly, and rearrangement upon lateral forces [25,26]. The adsorption and interfacial reorganization of globular proteins and microgels is schematically illustrated in Fig. 1.

2. Materials and methods

2.1. Materials

Table 1 reports the oils used in this study, with their interfacial tension against pure water (γ_{ow}). All oils were purified from polar contaminants with magnesium 70 silicate Florisil (MgO · SiO2, 100–200 mesh, Fluka Chemie GmbH, CH), as already described elsewhere [27].

The aqueous phase consisted of MilliQ-water (18.2 mΩcm) and 10 mM NaCl (Sigma Aldrich, >99.5 %). For the microgel synthesis and the single-particle analysis, the following chemicals were used: *N,N′*-methylenebis(acrylamide) (BIS, Fluka 99.0 %), methacrylic acid (MAA, Acros Organics 99.5 %), potassium persulfate (KPS, Sigma-Aldrich 99.0 %), isopropanol (Fisher Chemical, 99.97 %), toluene (Fluka Analytical, 99.7 %), *n*-hexane (SigmaAldrich, HPLC grade 95 %) and methyl *tert*-butyl ether (MTBE, SigmaAldrich, ACS reagent > 99.5 %) were used without further purification. N-isopropylacrylamide (NiPAM, TCI 98.0 %) was purified by recrystallization in 60/40 v/v toluene/hexane.

2.1.1. Microgels synthesis and characterization

pNIPAM (poly-*N*-isopropylacrylamide) microgels were synthesized with 5 mol % (stiffer microgels, D_h = 918 nm), or 1 mol % (softer microgels, D_h = 786 nm) *N*-*N*-methylenebisacrylamide (BIS) as cross-linker, and in addition copolymerized with 5 mol % methacrylic acid (MAA). The synthesis protocols are described in more detail in Vialetto et al. [28]. Their hydrodynamic diameter (D_h) is 918 ± 17 nm at T = 22 °C and 499 ± 2 nm at 40°C for the stiffer microgel and 786 ± 13 nm at T = 22 °C and 319 ± 1 nm at 40 °C for the softer microgel (Zetasizer, Malvern). Before the experiments, we purified the microgels suspension by centrifugation and supernatant exchange with pure water. This was repeated until the interfacial tension of the supernatant, as measured via bubble pressure tensiometry, reached a value close to the one of pure water (72.8 mN/m).

2.2. Methods

2.2.1. Pendant drop tensiometry

A drop profile tensiometer (PAT-1, SINTERFACE Technologies, Germany) was used for interfacial tension measurements, microgels adsorption kinetics, and dilatational rheology measurements, as described in detail by Loglio et al. [29]. We formed a droplet of microgel solution (500 mg/L and 10 mM NaCl) in pure oil at the tip of a capillary. Preceding the experiment, we tested each oil against water to confirm a correct and constant γ_{ow} and ensure the oil’s purity. Axisymmetric drop shape analysis was employed to determine the interfacial tension from the contour of the drop monitored by a CCD camera. For particles to adsorb completely and the interfacial layer to reach equilibrium, the droplet was kept constant for 20 h. Following, we performed a dilatation amplitude sweep. Each oscillation cycle was performed for 30 min at a constant frequency of $\omega = 0.01\ s^{-1}$. The drop was left at a constant area for 20 min between the oscillations to reach an equilibrated shape. The strain modulus E′ was derived based on Rühs et al. [30] at the area change ΔA/A = 2 %.

Table 1
List of all the oils used, featuring their interfacial tension and purity.

Oil	γ_{ow} [mN/m]	Purity [%]	Company
n-Octane	50.0	≥99 %	Fisher Chemical, Germany
n-Hexane	50.4	≥97 %	Sigma Aldrich, France
1-Chlorooctane	36.0	99 %	Alfa Aesar, Germany
1-Octanol	7.8	≥99 %	Sigma Aldrich, USA
Toluene	36.8	≥99 %	Merck KGaA, Germany
MCT (Myritol 318)	28.0	N.A.	BASF, Germany
MTBE (Methyl *tert*-butyl ether)	9.8	100 %	VWR Chemicals, France

2.2.2. Single-particles analysis

Isolated microgels were deposited onto silicon wafers from the fluid interface for atomic force microscopy (AFM) imaging following an already-reported procedure [26,28]. After cutting the silicon wafers into pieces, they were cleaned for 15 min by ultrasonication in solvents (toluene, isopropanol, acetone, ethanol, and MilliQ-water). A silicon wafer was fixed to a linear motion driver and immersed in water inside a Teflon beaker.. We formed the *n*-hexane, toluene, or MTBE interface to water subsequently. Approximately 10 μL microgel suspension (4:1 water: isopropanol solution) were injected at the interface, and after an equilibration time of 10 min, the silicon wafers were extracted vertically at a speed of 25 μm s^{-1}. During the crossing of the fluid interfaces, the adsorbed microgels were collected. Thereafter, the microgel-covered wafers were imaged with an AFM (Bruker Icon Dimension) in tapping mode using cantilevers with ~300 kHz resonance frequency and ~26 mN m^{-1} spring constant (OMCLAC160TS-R3, Olympus). Height and phase images were recorded simultaneously. We firstly processed images with Gwyddion. After, images are analyzed with a custom MATLAB code to obtain the average microgel height profile. A horizontal and vertical height profile through the center was measured and averaged over 20 microgels for each analyzed microgel. Next, we determined the diameter by fitting a circle on the microgels in the phase images. Lastly, we measured the core diameter by setting a lower threshold of 2.5 nm in the height profiles. We then used this to calculate the lateral extension of the microgel corona (corona width).

3. Results and discussions

To outline the extent of the similarity between proteins and microgels at fluid interfaces, we compare the following aspects: (i) their adsorption behavior and interfacial pressure build-up, (ii) their dilatational rheology, and (iii) their size and shape after adsorption and denaturing/spreading.

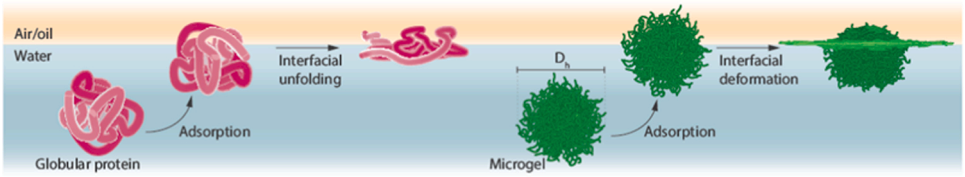

Fig. 1. Schematic illustration of the adsorption and interfacial deformation (spreading) of a globular protein and a pNIPAM microgel at an oil-water or air-water interface.

To elucidate the first aspect, we measured the spontaneous, diffusion-controlled adsorption of two different microgels (a “softer" and a “stiffer" one, having 1 or 5 mol % of *N-N*-methylenebisacrylamide (BIS) as cross-linker, respectively) with the pendant drop technique by monitoring the profile of an aqueous droplet (containing the microgels) in oils with different initial interfacial tension γ_{ow}. The adsorption starts at an interfacial pressure $\Pi = 0$ and the adsorbing microgels increase Π to a final, steady-state, interfacial pressure $\Pi_\infty = \gamma_{ow} - \gamma_\infty$, with γ_∞ being the equilibrated interfacial tension, as shown in the Supporting information Figure S1. The increase in Π originates from the adsorption of microgels to the interface and the subsequent spreading of surface-active polymer chains, which results in a decrease of the interfacial energy. Higher values of γ_{ow} cause stronger lateral deformation forces on the adsorbed particles, resulting in a faster and more pronounced spreading at the interface [28,31]. Furthermore, the adsorption of microgels depends on the diffusive and convective mass transport to the interface as well as on the presence of energetic barriers [19], analogously to the case of globular proteins [9]. The initial concentration affects mass transport, and the adsorption barriers depend on the interfacial coverage, with high interfacial coverage reducing the adsorption rate [32]. Hence, globular protein adsorb faster to fluid interfaces than microgels (see the interfacial diffusion coefficient in Supplementary information Figure S2), presumably due to their significantly smaller radii, and consequently increased bulk diffusion coefficient.

To compare the equilibrium adsorption at different oil interfaces, the values of Π_∞ are plotted as a function of γ_{ow}, as shown in Fig. 2 [8,17,24,33,34]. The lowest Π_∞ is found at the 1-octanol-water interface, which has the lowest γ_{ow}. For interfaces with increasing γ_{ow}, Π_∞ rises as a power-law with an exponent a:

$$\Pi_\infty \propto \gamma_{ow}^{a} \tag{1}$$

Both microgels reveal an exponent $a = 1.5$. In comparison to other adsorbing substances such as surfactants ($a = 1$) [34], flexible protein ($a = 1.25$) [24], and noncrystalline cellulose ($a = 3$) [33], microgels closely resemble the behavior of globular proteins, which also show $a = 1.5$. In both cases, it is hypothesized that the exponent of 1.5 originates from a dependency on the lateral interfacial forces, which unfold and flatten the proteins and the microgels at the interface [10,24].

After examining adsorption, we move to the characterization of the dilatation storage (E′) and loss (E”) moduli, which describe the 2D viscoelastic response upon compression and expansion of the adsorbed microgel monolayers. To assess the mechanical properties of the monolayers as a function of the interfacial tension of the fluid interface, E′ and E” were measured with the pendant drop tensiometer after the interface reached steady-state ($\Pi = \Pi_\infty$).

All interfacial layers exhibit predominately elastic properties, i.e., E′ > E”. For simplicity reasons, Fig. 3 only depicts E′ as a function of γ_{ow}. For the stiffer microgels, the elasticity of the interfacial layers increases slightly with higher γ_{ow}, due to increasing deformation. The increased deformation results in larger particle diameters, thereby increasing microgel contact at the interface and providing more resistance to mechanical stress [35]. The softer microgels’ viscoelastic response to dilatation is weaker than the one measured for the stiffer microgels. Additionally, E′ remained essentially unaffected by the nature of the oil phase, maintaining an approximately constant value of E′ ≈ 4 mN/m. The softer microgels have a significantly larger corona width, as shown in Vialetto et al. [28]. Hence, the loose corona polymers dominate the mechanical interaction between the individual soft microgels. Such interpretation is supported by the values E′ of the linear pNIPAM polymer, which is in a similar range as the softer microgels, especially at high γ_{ow}, where the softer microgels are stretched more.

Fig. 3 also contains literature results from globular and flexible proteins [8,10]. The comparison clearly shows that E′ is distinctly lower for the microgels. The elastic moduli of the measured microgels are instead in the range of flexible proteins, which suggests that the loose polymer coronas govern the 2D mechanical interactions for spontaneously adsorbed monolayers. Increasing the interfacial microgel density by compression increases the core to core contacts and might increase the similarity of the interfacial rheological behavior of microgels and globular proteins. Pinaud et al. [20] in fact measured dilatational moduli of microgels at the *n*-hexadecane-water interfaces in a similar range as found for globular proteins.

Whether cross-linking between proteins in interfacial layers plays a dominant role or not in the defining the mechanical response has not been fully unraveled yet. Dickinson and Matsumura [36] have proposed that strong covalent bonds enforce interactions in globular protein layers. However, recent works [10,37] indicate that disulfide bonds play a minor role in the formation of uniform and elastic interfacial networks with commonly used proteins such as β-lactoglobulin and lysozyme. To this end, in-situ cross-linking of microgels at interfaces could in the future offer a promising test to verify the role of chemical bonds in the

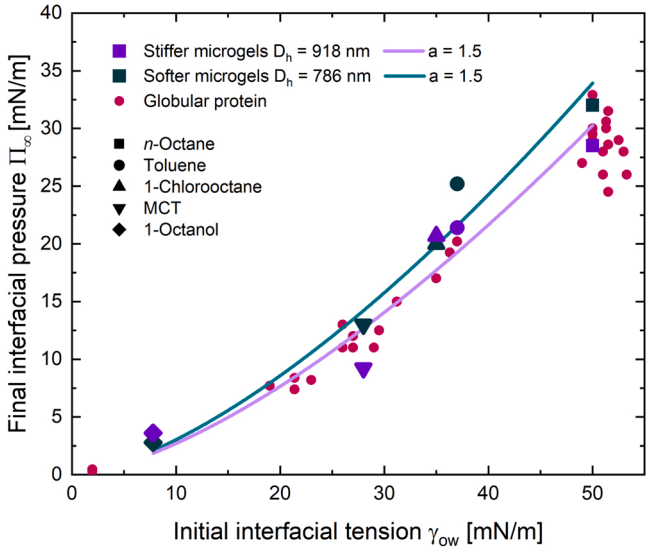

Fig. 2. Final interfacial pressure as a function of the initial interfacial tension for both microgel types and different oil-water interfaces compared to data of globular proteins redrawn from Ref. [17,24].

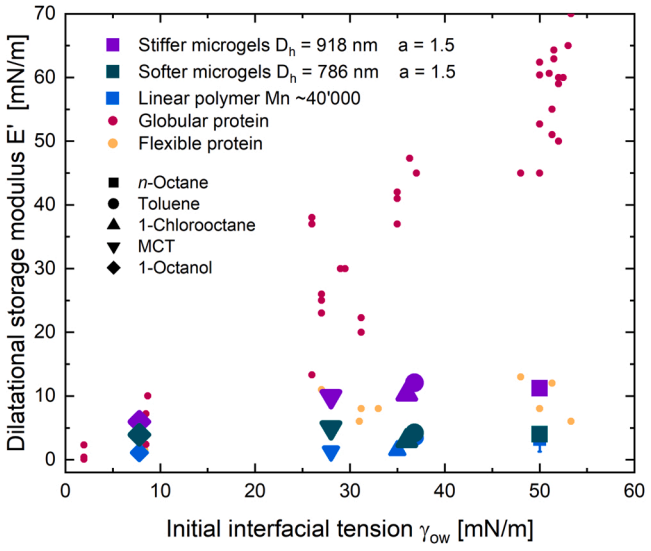

Fig. 3. Elastic dilatational modulus E′ of microgels plotted as a function of γ_{ow} for various o/w interfaces.

interfacial rheology of globular proteins.

Finally, moving on to the conformation of single objects at the interface, the choice of existing methods to elucidate the structural rearrangements of single proteins at oil-water interfaces is limited and available techniques either measure the degree of unfolding indirectly or quantify average thickness and roughness of the whole interface [8]. Conversely, single-particle characterization via atomic force microscopy has been shown for microgels after adsorption at the interface and subsequent deposition onto solid substrates [28]. Fig. 4, combines AFM data for microgels and literature results for two different kinds of globular proteins in the case of two interfaces with low γ_{ow} and high γ_{ow}, respectively. Fig. 4A reports the particle dry height for the same microgels used in this study after adsorption to a *n*-hexane-water interface (γ_{ow} = 50 mN/m) and a methyl tert-butyl ether (MTBE)-water interface (γ_{ow} = 10 mN/m). Even if the two microgels have slightly different dimensions in bulk (918 nm for the stiffer microgels and 786 nm for the softer microgels), the height difference after deposition from the interface is exacerbated due to the variation in cross-linking density. For both microgels, the height is significantly reduced at the high-γ_{ow} interface compared to low-γ_{ow}. A similar trend was found for globular proteins, as shown in Fig. 4B, with data based on interfacial globular protein layer thickness results from neutron reflectometry of β-lactoglobulin (BLG) layers from Bergfreund et al. [10] and dynamic force microscopy of bovine serum albumin (BSA) layers from Jia et al. [12]. Here, the main difference between BLG and BSA originates from the larger initial native size of BSA compared to BLG [10]. Bergfreund et al. [10] performed the BLG measurements with *n*-hexane and MTBE. Whereas for the BSA height measurements, perfluorodecalin was used as the high-γ_{ow} oil (γ_{ow} = 56.6 mN/m [38]) and perfluorotributylamine was used as low-γ_{ow} oil (γ_{ow} = 16 mN/m [39]). Similarly to the microgels, the interfacial height of globular proteins reduces by approximately 50 % at the high-γ_{ow} interfaces compared to the low-γ_{ow} interfaces. This findings are schematically illustrated in Fig. 4C and D.

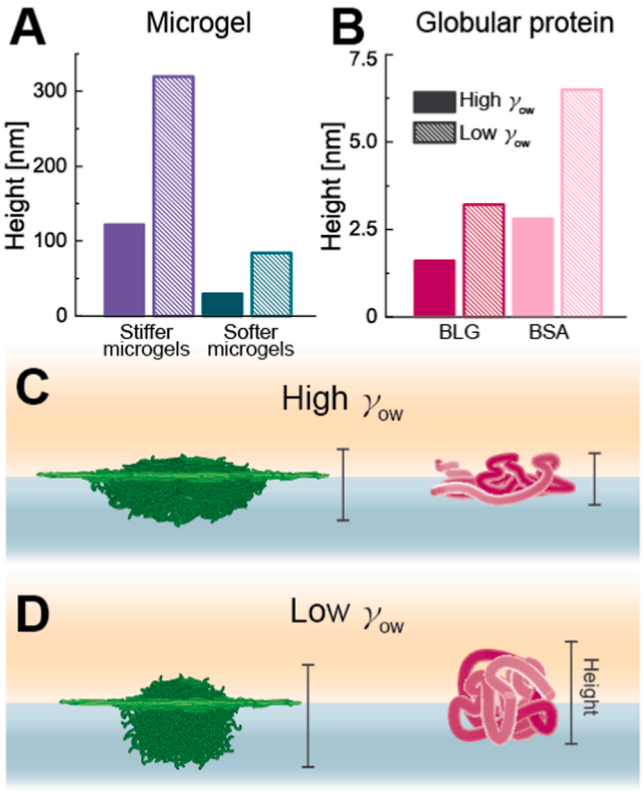

Fig. 4. Height of (A) stiffer and softer microgels after adsorption to *n*-hexane-water (high γ_{ow}) and MTBE-water (low γ_{ow}) interfaces and (B) globular proteins, BLG adsorbed at *n*-hexane-water and MTBE-water interfaces and BSA at perfluorodecalin-water (high γ_{ow}) and perfluorotributylamine (low γ_{ow}) interfaces. Schematic illustration of microgels and globular proteins at (C) high-γ_{ow} and (D) low-γ_{ow} interfaces. (A) contains data taken from Vialetto et al. [28] and (B) contains data taken from Bergfreund et al. [10] and Jia et al. [12].

In comparison to the relative simplicity of microgels, the highly structured morphology of globular proteins with secondary and tertiary structures leads to a more defined unfolding. For instance, Zare et al. [13] computed with molecular dynamic simulations that at non-polar oil-water interfaces, such as *n*-alkane-water, BLG adsorbs in a distinct orientation and open its cavity with the hydrophobic residues toward the oil phase. At polar o/w interfaces, such as triglycerides and 1-octanol, BLG adsorbs in a random orientation and retains a more native structure according to simulations [13]. Highly stable globular proteins, such as lysozyme and plant-based proteins, preserve a more native structure even at non-polar o/w interface [7,10,40]. Nevertheless, analysis of the secondary structure shows a slight decrease of α-helices upon adsorption [40], which indicates an increase in randomly folded peptide chain parts that probably are spread by the interfaces and assemble as a corona. This behavior is similar to the less cross-linked outer polymer chains of the microgels, which are capable of more significant distortion upon adsorption [23,26].

Contrary to hard particles, surrounding solvent molecules penetrate microgels and globular proteins [41,42]. The penetration of the solvents into the porous microgel and globular protein structures depends on the interaction of the polymer chains with the solvents. Strong interactions result in swelling, well described for microgels by the Hansen and Hildebrand parameter [28,43]. The different solubility in each solvent results in a distinct interfacial positioning and swelling on each side of the interface. Nevertheless, defining a contact angle for microgels and globular proteins is elusive, due to the high porosity and conformation [19]. Zare et al. [13] showed with molecular dynamic simulations that with increasing oil polarity, globular proteins increase the interactions with the oil molecules and bury themselves in the oil phase, which is in line with neutron reflectometry results [10]. Finally, microgels and globular proteins have different conformational changes at elevated temperatures. Dan et al. [16] pointed out that microgels shrink upon heating whereas globular proteins unfold. Even though both conformational changes result in increased interfacial activity, the adsorption mechanisms and interfacial behavior are different.

4. Conclusion

In summary, we have demonstrated the existence of similarities between pNIPAM microgels and globular proteins at fluid interfaces and emphasized their differences. A broad variety exists in terms of protein conformations, and in the shape and density profiles of microgels, which can be controlled during synthesis [25,26,44] enabling the selection of promising and relevant model systems. In particular, the steady-state interfacial pressures of two different pNIPAM microgels upon spontaneous adsorption to different o/w interfaces follow the same correlation as the one of globular proteins. However, the dilatational rheology of spontaneously adsorbed microgel interfaces differs significantly from the one of globular proteins monolayers, due to the dominating effect of the microgel's polymer corona in their mechanical response. Finally, the morphological interfacial rearrangements of microgels strongly depend on the γ_{ow}, as in the case of globular proteins, even though the high complexity of their internal structure results in a protein-specific unfolding, in particular at high-γ_{ow}. Microgels and most globular proteins reveal a similar reduction in their interfacial height, as they flatten more with increasing γ_{ow} due to stronger lateral forces. Concluding, to date, even if pNIPAM microgels cannot resemble the fine details of structure-defined adsorption orientation and unfolding processes found with globular proteins, they present interesting analogies. Synthesis of new anisotropic and heterogeneous microgels could further extend their characteristics towards the ones of globular proteins and strengthen their role as models systems for complex behavior.

CRediT authorship contribution statement

NN, JB, and JVdesigned and conducted experiments. NN and JB analysed and visualized data. NN,JB wrote initial manuscript. JB, JV, LI and PF reviewed and editedmanuscript. JB, PF and LI concepted research. PF and LI acquired funding and administeredproject.

Declaration of Competing Interest

The authors declare that they have no known competing financial interests or personal relationships that could have appeared to influence the work reported in this paper.

Acknowledgements

We acknowledge Pascal Bertsch for helpful discussions. The authors gratefully acknowledge support by the Swiss National Science Foundation (Grant #: 200021-175994). J.V. acknowledges funding from the European Union's Horizon 2020 Research and Innovation Program under Marie Skłodowska Curie grant agreement 888076.

Appendix A. Supporting information

Supplementary data associated with this article can be found in the online version at doi:10.1016/j.colsurfb.2022.112595.

References

[1] R. Mezzenga, P. Fischer, The self-assembly, aggregation and phase transitions of food protein systems in one, two and three dimensions, Rep. Prog. Phys. 76 (2013), 046601.
[2] E. Dickinson, Adsorbed protein layers at fluid interfaces: interactions, structure and surface rheology, Colloids Surf. B: Biointerfaces 15 (1999) 161–176.
[3] T.A. Khan, H.-C. Mahler, R.S. Kishore, Key interactions of surfactants in therapeutic protein formulations: a review, Eur. J. Pharm. Biopharm. 97 (2015) 60–67.
[4] P. Bertsch, J. Bergfreund, E.J. Windhab, P. Fischer, Physiological fluid interfaces: functional microenvironments, drug delivery targets, and first line of defense, Acta Biomater. 130 (2021) 32–53.
[5] P.A. Rühs, J. Bergfreund, P. Bertsch, S.J. Gstöhl, P. Fischer, Complex fluids in animal survival strategies, Soft Matter 17 (2021) 3022–3036.
[6] I.R. Jenkinson, L. Seuront, H. Ding, F. Elias, L. Thomsen, Biological modification of mechanical properties of the sea surface microlayer, influencing waves, ripples, foam and air-sea fluxes, Elem.: Sci. Anthr. 6 (2018) 26.
[7] L. Böcker, P. Bertsch, D. Wenner, S. Teixeira, J. Bergfreund, S. Eder, P. Fischer, A. Mathys, Effect of Arthrospira platensis microalgae protein purification on emulsification mechanism and efficiency, J. Colloid Interface Sci. 584 (2021) 344–353.
[8] J. Bergfreund, P. Bertsch, P. Fischer, Effect of the hydrophobic phase on interfacial phenomena of surfactants, proteins, and particles at fluid interfaces, Curr. Opin. Colloid Interface Sci. 56 (2021), 101509.
[9] V. Mitropoulos, A. Mütze, P. Fischer, Mechanical properties of protein adsorption layers at the air/water and oil/water interface: a comparison in light of the thermodynamical stability of proteins, Adv. Colloid Interface Sci. 206 (2014) 195–206.
[10] J. Bergfreund, M. Diener, T. Geue, N. Nussbaum, N. Kummer, P. Bertsch, G. Nyström, P. Fischer, Globular protein assembly and network formation at fluid interfaces: effect of oil, Soft Matter (17) (2021) 1692–1700.
[11] J. Zhai, T.J. Wooster, S.V. Hoffmann, T.-H. Lee, M.A. Augustin, M.-I. Aguilar, Structural rearrangement of β -lactoglobulin at different oil-water interfaces and its effect on emulsion stability, Langmuir 27 (2011) 9227–9236.
[12] X. Jia, K. Minami, K. Uto, A.C. Chang, J.P. Hill, T. Ueki, J. Nakanishi, K. Ariga, Modulation of mesenchymal stem cells mechanosensing at fluid interfaces by tailored self-assembled protein monolayers, Small 15 (2019), 1804640.
[13] D. Zare, J.R. Allison, K.M. McGrath, Molecular dynamics simulation of β -lactoglobulin at different oil/water interfaces, Biomacromolecules 17 (2016) 1572–1581.
[14] W. Liao, Y. Zhang, Y. Guan, X. Zhu, Gelation kinetics of thermosensitive PNIPAM microgel dispersions, Macromol. Chem. Phys. 212 (2011) 2052–2060.
[15] W. Liao, Y. Zhang, Y. Guan, X. Zhu, Fractal structures of the hydrogels formed in situ from poly (N-isopropylacrylamide) microgel dispersions, Langmuir 28 (2012) 10873–10880.
[16] A. Dan, P. Agnihotri, S. Bochenek, W. Richtering, Adsorption dynamics of thermoresponsive microgels with incorporated short oligo (ethylene glycol) chains at the oil-water interface, Soft Matter (2021) 17.
[17] J. Bergfreund, P. Bertsch, S. Kuster, P. Fischer, Effect of oil hydrophobicity on the adsorption and rheology of β -lactoglobulin at oil-water interfaces, Langmuir 34 (2018) 4929–4936.
[18] Z. Li, K. Geisel, W. Richtering, T. Ngai, Poly(N-isopropylacrylamide) microgels at the oil-water interface: adsorption kinetics, Soft Matter 9 (2013) 9939–9946.
[19] B.S. Murray, Microgels at fluid-fluid interfaces for food and drinks, Adv. Colloid Interface Sci. 271 (2019), 101990.
[20] F. Pinaud, K. Geisel, P. Massé, B. Catargi, L. Isa, W. Richtering, V. Ravaine, V. Schmitt, Adsorption of microgels at an oil-water interface: correlation between packing and 2D elasticity, Soft Matter 10 (2014) 6963–6974.
[21] S. Wongsuwarn, D. Vigolo, R. Cerbino, A.M. Howe, A. Vailati, R. Piazza, P. Cicuta, Giant thermophoresis of poly (N-isopropylacrylamide) microgel particles, Soft Matter 8 (2012) 5857–5863.
[22] M. Stieger, W. Richtering, J.S. Pedersen, P. Lindner, Small-angle neutron scattering study of structural changes in temperature sensitive microgel colloids, J. Chem. Phys. 120 (2004) 6197–6206.
[23] F. Camerin, M.A. Fernández-Rodríguez, L. Rovigatti, M.-N. Antonopoulou, N. Gnan, A. Ninarello, L. Isa, E. Zaccarelli, Microgels adsorbed at liquid-liquid interfaces: a joint numerical and experimental study, ACS Nano 13 (2019) 4548–4559.
[24] J. Bergfreund, P. Bertsch, P. Fischer, Adsorption of proteins to fluid interfaces: role of the hydrophobic subphase, J. Colloid Interface Sci. 584 (2021) 411–417.
[25] J. Hegemann, H.-H. Boltz, J. Kierfeld, Elastic capsules at liquid-liquid interfaces, Soft Matter 14 (2018) 5665–5685.
[26] J. Vialetto, F. Camerin, F. Grillo, S.N. Ramakrishna, L. Rovigatti, E. Zaccarelli, L. Isa, Effect of internal architecture on the assembly of soft particles at fluid interfaces, ACS Nano 15 (2021) 13105–13117.
[27] K. Mishra, J. Bergfreund, P. Bertsch, P. Fischer, E.J. Windhab, Crystallization-induced network formation of tri-and monopalmitin at the middle-chain triglyceride oil/air interface, Langmuir 36 (2020) 7566–7572.
[28] J. Vialetto, N. Nussbaum, J. Bergfreund, P. Fischer, L. Isa, Influence of the interfacial tension on the microstructural and mechanical properties of microgels at fluid interfaces, J. Colloid Interface Sci. 608 (2022) 2584–2592.
[29] G. Loglio, P. Pandolfini, R. Miller, A. Makievski, F. Ravera, L. Liggieri, Drop and bubble shape analysis as a tool for dilational rheological studies of interfacial layers, in: D. Möbius, R. Miller (Eds.), Novel Methods to Study Interfacial Layers, Elsevier, Amsterdam, 2001, pp. 439–483.
[30] P.A. Rühs, C. Affolter, E.J. Windhab, P. Fischer, Shear and dilatational linear and nonlinear subphase controlled interfacial rheology of β -lactoglobulin fibrils and their derivatives, J. Rheol. 57 (2013) 1003–1022.
[31] R.W. Style, L. Isa, E.R. Dufresne, Adsorption of soft particles at fluid interfaces, Soft Matter 11 (2015) 7412–7419.
[32] O.S. Deshmukh, A. Maestro, M.H. Duits, D. Van Den Ende, M.C. Stuart, F. Mugele, Equation of state and adsorption dynamics of soft microgel particles at an air-water interface, Soft Matter 10 (2014) 7045–7050.
[33] J. Bergfreund, Q. Sun, P. Fischer, P. Bertsch, Adsorption of charged anisotropic nanoparticles at oil-water interfaces, Nanoscale Adv. 1 (2019) 4308–4312.
[34] J. Bergfreund, S. Siegenthaler, V. Lutz-Bueno, P. Bertsch, P. Fischer, Surfactant adsorption to different fluid interfaces, Langmuir (2021) 37.
[35] M. Destribats, V. Lapeyre, E. Sellier, F. Leal-Calderon, V. Ravaine, V. Schmitt, Origin and control of adhesion between emulsion drops stabilized by thermally sensitive soft colloidal particles, Langmuir 28 (2012) 3744–3755.
[36] E. Dickinson, Y. Matsumura, Time-dependent polymerization of β -lactoglobulin through disulphide bonds at the oil-water interface in emulsions, Int. J. Biol. Macromol. 13 (1991) 26–30.
[37] H. Schestkowa, S. Drusch, A.M. Wagemans, FTIR analysis of β -lactoglobulin at the oil/water-interface, Food Chem. 302 (2020), 125349.
[38] N. Nishikido, W. Mahler, P. Mukerjee, Interfacial tensions of perfluorohexane and perfluorodecalin against water, Langmuir 5 (1989) 227–229.
[39] S. Chang, N.J. Zimmerman, T. Iwamoto, R. Ortiz, D. Faris, Experimental vitreous replacement with perfluorotributylamine, Am. J. Ophthalmol. 103 (1987) 29–37.
[40] L. Day, J. Zhai, M. Xu, N.C. Jones, S.V. Hoffmann, T.J. Wooster, Conformational changes of globular proteins adsorbed at oil-in-water emulsion interfaces examined by synchrotron radiation circular dichroism, Food Hydrocoll. 34 (2014) 78–87.
[41] R.A. Gumerov, A.M. Rumyantsev, A.A. Rudov, A. Pich, W. Richtering, M. Möller, I. I. Potemkin, Mixing of two immiscible liquids within the polymer microgel adsorbed at their interface, ACS Macro Lett. 5 (2016) 612–616.
[42] S. Damodaran, L. Razumovsky, Role of surface area-to-volume ratio in protein adsorption at the air-water interface, Surf. Sci. 602 (2008) 307–315.
[43] T. Hoare, R. Pelton, Functionalized microgel swelling: comparing theory and experiment, J. Phys. Chem. B 111 (2007) 11895–11906.
[44] A.C. Nickel, T. Kratzenberg, S. Bochenek, M.M. Schmidt, A.A. Rudov, A. Falkenstein, I.I. Potemkin, J.J. Crassous, W. Richtering, Anisotropic microgels show their soft side, Langmuir (2021).